Superfluid state of atomic ^{6}Li in a magnetic trap

M. Houbiers, R. Ferwerda, and H. T. C. Stoof

Institute for Theoretical Physics, University of Utrecht, P.O. Box 80 006, 3508 TA Utrecht, The Netherlands

W. I. McAlexander, C. A. Sackett, and R. G. Hulet

Physics Department and Rice Quantum Institute, Rice University, Houston, Texas 77005

We report on a study of the superfluid state of spin-polarized atomic ^{6}Li confined in a magnetic trap. Density profiles of this degenerate Fermi gas and the spatial distribution of the BCS order parameter are calculated in the local-density approximation. The critical temperature is determined as a function of the number of particles in the trap. Furthermore, we consider the mechanical stability of an interacting two-component Fermi gas, in the case of both attractive and repulsive interatomic interactions. For spin-polarized ^{6}Li we also calculate the decay rate of the gas and show that within the mechanically stable regime of phase space, the lifetime is long enough to perform experiments on the gas below and above the critical temperature if a bias magnetic field of about 5 T is applied. Moreover, we propose that a measurement of the decay rate of the system might signal the presence of the superfluid state. [S1050-2947(97)06512-8]

I. INTRODUCTION

One of the most important objectives in the study of dilute gases has been the achievement of Bose-Einstein condensation (BEC) in bosonic systems. Indeed, decades of experimental research finally led two years ago to the observation of BEC in three different systems of alkali-metal gases ^{87}Rb, ^{7}Li, and ^{23}Na [1–3]. This success has triggered a large amount of interest in the field of ultracold atomic gases. Although the study of properties of these degenerate atomic Bose gases is vigorously being pursued at the moment, trapping and cooling of Fermi gases might also provide new and exciting physics. Indeed, in a previous theoretical study we showed that a gas of spin-polarized atomic ^{6}Li becomes superfluid at densities and temperatures comparable with those at which the Bose-Einstein experiments are performed [4].

This superfluid phase transition, which is similar to the BCS transition in a superconductor, occurs at such high temperatures due to the fact that ^{6}Li has an anomalously large and negative (triplet) s-wave scattering length a [5]. This scattering length is a measure for the interatomic interactions and its sign implies that this interaction is effectively attractive, which is a first requirement for a BCS transition to occur. For other atomic species, the transition temperature is in general very low because the scattering length is of the order of the range of the interaction r_V and the diluteness of the gas requires that the Fermi wave number $k_F \ll 1/r_V$. So, for example, in the case of deuterium, it was concluded already some time ago that the observation of a BCS transition is experimentally impossible [6].

The ^{6}Li atom has nuclear spin $i=1$ and electron spin $s=1/2$. Consequently, the atom has six hyperfine states $|1\rangle$–$|6\rangle$, for which the level splitting in a magnetic field is shown in Fig. 1. The upper three levels $|4\rangle$–$|6\rangle$ can be trapped in a static magnetic trap, whereas the lowest three hyperfine levels prefer high magnetic fields and are expelled from a magnetic-field minimum.

The simplest way to create a degenerate Fermi gas is to trap just one low-field seeking hyperfine state, and for the sake of stability of the gas, the doubly polarized state $|6\rangle = |m_s = 1/2, m_i = 1\rangle$ is most suitable. However, due to the Pauli exclusion principle, two fermions in the same hyperfine state can interact with each other at best via p waves, and if this interaction is effectively attractive, the onset of the formation of Cooper pairs occurs at a temperature

$$T_c \simeq \frac{\epsilon_F}{k_B} \exp\left\{ -\frac{\pi}{2(k_F|a|)^3} \right\},$$

where $\epsilon_F = \hbar^2 k_F^2/2m$ is the Fermi energy of the atomic gas and a the p-wave scattering length. For ^{6}Li this p-wave scattering length of the triplet potential is approximately $-35a_0$, where a_0 is the Bohr radius, and $k_F a \ll 1$ in general. As a result, the critical temperature for such a doubly spin-polarized ^{6}Li gas is extremely low. At present, a reasonable number for the density of trapped atomic gases is 10^{12} cm^{-3}, leading to $\epsilon_F/k_B \simeq 600$ nK and $k_F|a| \simeq 7 \times 10^{-3}$. The corresponding critical temperature is clearly unattainable.
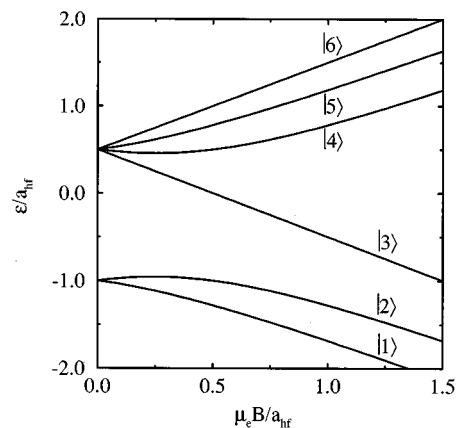

FIG. 1. Energy of the six hyperfine states of ^{6}Li in units of the hyperfine constant a_{hf}, as a function of the magnetic field.

In the case that more than one state is trapped, Baranov *et al.* [7] predicted a considerable increase in the above (*p*-wave) critical temperature as a result of the fact that two atoms in the same spin state can now also attract each other through the exchange of a phonon (density fluctuation) in another hyperfine state. It was found that in this case the transition temperature

$$T_c \simeq \frac{\epsilon_F}{k_B} \exp\left\{ -13\left(\frac{\pi}{2k_F|a|}\right)^2 \right\},$$

where *a* now corresponds to the *s*-wave scattering length for collisions between the two hyperfine states. Nevertheless, using again a density of 10^{12} cm^{-3} for each spin state and the value $a = -2160a_0$ for ^{6}Li [5], we find that $k_F|a| \simeq 0.43$ and it is easily verified that also in this case the critical temperature is out of reach experimentally.

Therefore, the most promising approach is to consider a Cooper pair of two atoms in different hyperfine states since then *s*-wave pairing is allowed. In this case [8]

$$T_c \simeq \frac{\epsilon_F}{k_B} \exp\left\{ -\frac{\pi}{2k_F|a|} \right\},$$

resulting in a much higher critical temperature than in the previous two cases. In particular, we envision to trap ^{6}Li atoms in the states $|6\rangle$ and $|5\rangle$. Experimentally, this might be achieved most easily by first trapping only one hyperfine level and then applying a *noisy* rf pulse to create an incoherent mixture of atoms occupying these two hyperfine levels [9]. Note that this situation has in fact already been realized in recent experiments with ^{87}Rb atoms, although using a different technique [10].

In a recent work Modawi and Leggett propose to trap ^{6}Li atoms in three instead of two hyperfine states [11]. The advantage in such a system is that the effect of fluctuations is reduced somewhat, but the disadvantage of trapping more hyperfine states is that the number of channels by which the gas can decay increases considerably. There are not only more possibilities for two-body collision processes, in which one or two electron spins are flipped and the corresponding atoms are expelled from the trap, but also three-body recombination processes are now no longer suppressed. Therefore, at present, it seems to be most favorable to trap only two hyperfine states and the most suitable candidates are the states $|6\rangle = |m_s = 1/2; m_i = 1\rangle$ and $|5\rangle \simeq |m_s = 1/2; m_i = 0\rangle$ because for this combination the decay processes due to two-body interactions can be suppressed most. The approximate sign in the second expression indicates that in the state $|5\rangle$ there is for $\mu_e B \gg a_{hf}$ a small admixture with the spin state $|m_s = -1/2; m_i = 1\rangle$. Although this admixture can be neglected for most purposes, we will return to its importance for the stability of the gas shortly.

As explained above, in a two-component spin-polarized atomic ^{6}Li gas, Cooper pairing will occur only between atoms in different spin states, while there is almost no interaction between two atoms in the same spin states. For notational simplicity, we also refer to these states as $|\uparrow\rangle$ and $|\downarrow\rangle$ and the densities of atoms in these two hyperfine states are denoted by $n_\uparrow$ and $n_\downarrow$, respectively. Notice that since the two states are electron-spin polarized, the strength of the inter-

atomic interaction is indeed characterized by the *s*-wave scattering length of the triplet potential $V_T(\mathbf{r})$ and it is exactly this number that is anomalously large and negative in the case of ^{6}Li.

The aim of the present paper is threefold. First, the homogeneous calculation of Ref. [4] needs some improvement due to the fact that the interatomic interaction potential for ^{6}Li has recently been determined more accurately [5]. The most up-to-date value of the *s*-wave scattering length is $a = -2160a_0$, where a_0 is the Bohr radius. This change in *a* affects not only the critical temperature but also the decay rates of the gas. Second, we want to take the effect of the inhomogeneity of the trapped gas into account. Third, we look for a signature that signals the presence of the superfluid phase in the gas.

The paper is organized as follows. In Sec. II A we consider in some detail the decay processes limiting the lifetime of the gas. Subsequently, we briefly summarize the theory for the homogeneous Fermi gas in Sec. II B and improve the results obtained earlier for the critical temperature, using the most up-to-date interatomic potential for ^{6}Li. In Sec. II C we consider the mechanical stability of a weakly interacting Fermi gas. In particular, we also consider a gas with positive *s*-wave scattering length and show that in the unstable part of the phase diagram, a spinodal decomposition can restore the stability of the gas in this case.

In future experiments the atoms are likely to be trapped in an external potential that roughly has the shape of an isotropic harmonic oscillator $V(\mathbf{r}) = \frac{1}{2} m \omega^2 \mathbf{r}^2$ and causes the gas cloud to be inhomogeneous. Therefore, Sec. III of this paper is devoted to the study of an inhomogeneous two-component Fermi gas at and below the critical temperature and in particular we will again concentrate on ^{6}Li. The numerical calculations will be performed in the local-density approximation, which is valid if the correlation length ξ over which the particles influence each other is much smaller than the typical trap size $l = \sqrt{\hbar/m\omega}$ over which the density of the gas changes. A similar calculation for the noninteracting case has been performed recently by Butts and Rokhsar [12]. In addition, the case of purely repulsive interactions has been studied by Oliva in the same way in the context of possible experiments with spin-polarized atomic deuterium [13]. In Sec. III A we briefly repeat the ingredients for the local-density approximation. In Sec. III B we calculate the critical temperature of the gas as a function of the number of trapped atoms and in Sec. III C we study the gas in the superfluid state. Density profiles for the gas as well as for the BCS order parameter are presented. In Sec. IV we devote a discussion to the issue of how to detect the superfluid phase and to distinguish it from the normal phase. We end the paper with a summary of the main conclusions.

II. HOMOGENEOUS FERMI GAS

We first consider a homogeneous, dilute gas of (electron-)spin-polarized ^{6}Li atoms. Since the gas is dilute, the atoms will interact with each other mainly through two-body collisions. These two-body collisions can be represented on the mean-field level by a local potential with a strength given by the two-body scattering matrix $T^{2B} = 4\pi a \hbar^2/m$, where *m* is the mass of the particles and *a* is the scattering length [14].

The sign of a determines whether the two-body interaction is effectively repulsive ($a>0$) or attractive ($a<0$).

Before going to a description of the gas in the normal and superfluid state, we consider an aspect that is experimentally of some importance, namely, the lifetime of the gas. The large s-wave scattering length has, on the one hand, the advantage of having many thermalizing collisions between the particles which is required for efficient evaporative cooling, but, on the other hand, there will also be relatively many inelastic collisions, which can cause spin flips within the atoms. If the electron spin of an atom is inverted, the atom will be lost from the trap and consequently these inelastic processes limit the lifetime of the gas. In the next subsection we explain in more detail which decay processes dominate in a mixture of ^{6}Li atoms in the hyperfine states $|6\rangle$ and $|5\rangle$.

A. Decay rates

The electron-spin and nuclear-spin quantum numbers of the two trapped hyperfine levels for $\mu_e B \gg a_{hf}$ are given by

$$|6\rangle = |m_s = 1/2; m_i = 1\rangle,$$

$$|5\rangle = |m_s = 1/2; m_i = 0\rangle + \theta^+ |m_s = -1/2; m_i = 1\rangle,$$

where $\theta^+ \simeq a_{hf}/2\sqrt{2}\mu_e B$ is inversely proportional to the applied magnetic field B, so for sufficiently strong magnetic fields the admixture of $|5\rangle$ with the high-field seeking part is small and the gas can considered to be electron-spin polarized. For such large magnetic fields, the energies of these two hyperfine levels are given by $\epsilon_6 = a_{hf}/2 + \mu_e B$ and $\epsilon_5 \simeq \mu_e B$, respectively.

Since the two atoms in states $|5\rangle$ and $|6\rangle$ will interact at the low temperatures of interest solely via s-wave scattering, implying that the spatial part of the two-body wave function is symmetric under the exchange of atoms, the spin part of the wave function must be antisymmetric, i.e.,

$$|\{6,5\}_-\rangle = \frac{1}{\sqrt{2}}[|6\rangle|5\rangle - |5\rangle|6\rangle] = |11;11\rangle + \theta^+|00;22\rangle,$$
$$(1)$$

where in the last line we used the basis $|SM_S; IM_I\rangle$ with $\mathbf{S} = \mathbf{s}_1 + \mathbf{s}_2$ and $\mathbf{I} = \mathbf{i}_1 + \mathbf{i}_2$ the total electron and nuclear spin of the two colliding atoms and M_S and M_I the corresponding magnetic quantum numbers along the direction of the magnetic field.

The decay rates for the transition from the state $|lm, \{\alpha, \beta\}\rangle$ with orbital quantum numbers l and m to a state $|l'm', \{\alpha', \beta'\}\rangle$ with quantum numbers l' and m' are essentially given by Fermi's golden rule and results in the expression [15]

$$G_{\alpha,\beta \to \alpha',\beta'}(B) = 2\pi^3 \hbar^2 m p_{\alpha',\beta'}$$
$$\times |T_{l'm'\{\alpha',\beta'\},lm\{\alpha,\beta\}}(p_{\alpha',\beta'},0)|^2 \quad (2)$$

for the zero-temperature limit of the rate constant for this process. Here $T_{l'm'\{\alpha',\beta'\},lm\{\alpha,\beta\}}(p_{\alpha',\beta'},0)$ is the two-body scattering matrix at zero energy such that the incoming particles have zero relative momentum and the magnitude of the relative momentum of the scattered particles is $p_{\alpha',\beta'}$.

As explained, for example, in Ref. [4], there are basically two ways in which collisions cause the atoms to be lost from the trap. First of all, the central (singlet and triplet) interaction $V^c = V_S(\mathbf{r})\mathcal{P}^{(S)} + V_T(\mathbf{r})\mathcal{P}^{(T)}$ induces transitions between different hyperfine levels. Since this interaction cannot change the total electron- or nuclear-spin angular momentum and the hyperfine level $|5\rangle$ has a small admixture with the state $|m_s = -1/2, m_i = 1\rangle$, only transitions $|\{6,5\}_-\rangle \to |\{6,1\}_-\rangle$, where $|1\rangle \simeq |m_s = -1/2, m_i = 1\rangle - \theta^+ |m_s = 1/2, m_i = 0\rangle$, are allowed. Similar to Eq. (1), the total spin state $|\{6,1\}_-\rangle$ is given by

$$|\{6,1\}_-\rangle = |00;22\rangle - \theta^+ |11;11\rangle. \quad (3)$$

Combining Eqs. (1) and (3), we find that the spin part of the transition matrix $T_{00\{6,1\},00\{6,5\}}(p_{61},0)$ contributes a factor θ^+ times the exchange potential $V^{ex}(\mathbf{r}) = V_T(\mathbf{r}) - V_S(\mathbf{r})$, i.e., the difference between the triplet and singlet potentials. To calculate the spatial part, we must use for the relative incoming and outgoing scattering wave functions with orbital quantum numbers l and m and total electron spin S the normalized expression

$$\Psi_{lmS}^{(\pm)}(\mathbf{r}) = \sqrt{\frac{2}{\pi\hbar^3}} \frac{\psi_{lS}^{(\pm)}(r)}{r} i^l Y_{lm}(\hat{\mathbf{r}}), \quad (4)$$

where $\psi_{lS}^{(\pm)}(r)$ denotes the incoming and outgoing solutions to the radial Schrödinger equation with the singlet or triplet interaction. Using furthermore that the relative momentum p_{61} after scattering is due to the energy difference $\epsilon_6 - \epsilon_1 = 2\mu_e B$, we find that $p_{61} = \sqrt{2m\mu_e B}$. Combining all expressions into Eq. (2), we obtain that the rate constant due to exchange interactions is given by

$$G^{ex} = 2\pi^3 \hbar^2 m p_{61}(\theta^+)^2$$
$$\times |\langle \Psi_{000}^{(-)}(\mathbf{r},p_{61})|V_T(\mathbf{r}) - V_S(\mathbf{r})|\Psi_{001}^{(+)}(\mathbf{r},0)\rangle|^2$$
$$= \pi^3 \hbar^2 \left(\frac{m}{2\mu_e B}\right)^{3/2} a_{hf}^2$$
$$\times |\langle \Psi_{000}^{(-)}(\mathbf{r},p_{61})|V^{ex}(\mathbf{r})|\Psi_{001}^{(+)}(\mathbf{r},0)\rangle|^2. \quad (5)$$

In Fig. 2 this exchange rate as a function of the magnetic field is shown (curve 1).

The second way in which collisions cause decay of the gas is due to magnetic dipolar interactions V^d. As will be shown, of the various dipolar interactions, the contribution due to electron-electron dipolar interactions is most important. For this dipolar interaction, we have [15]

$$V^d = -\frac{\mu_0 \mu_e^2}{4\pi r^3} \sqrt{\frac{4\pi}{5}} \sum_{\Delta M_S} (-1)^{\Delta M_S} Y_{2-\Delta M_S}(\hat{\mathbf{r}}) \Sigma_{2,\Delta M_S}^{ee},$$
$$(6)$$

where the tensor operator $\Sigma_{2,\Delta M_S}^{ee}$ can be thought of as arising from the coupling between $\mathbf{s}_1/\hbar$ and $\mathbf{s}_2/\hbar$, the Pauli spin matrices describing the electron spin of the two atoms, to a tensor of rank 2. For the scattering state $|\{6,5\}_-\rangle \simeq |11;11\rangle$, the dipolar interaction can change the (total) electron spin projection M_S of the two atoms by an amount $\Delta M_S = -1$ for
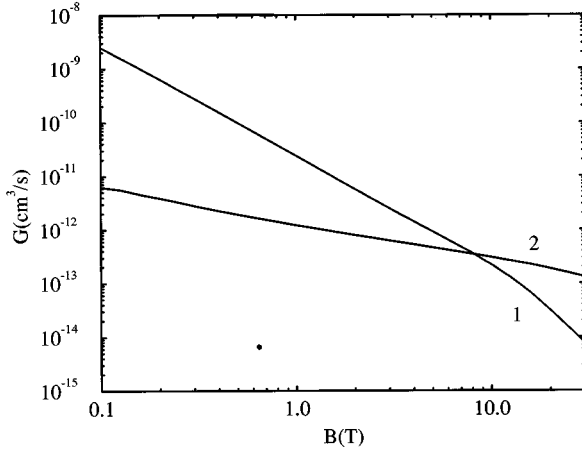
FIG. 2. Decay rate constants due to exchange (curve 1) and one-spin-flip processes (curve 2) as a function of the applied magnetic bias field.

a one-spin-flip $(1SF)$ or $\Delta M_S = -2$ for a two-spin-flip $(2SF)$ process. Therefore, the one- (two-) spin-flip dipolar interaction couples the incoming wave function with approximately $S=1, M_S=1$ to the final state having $S=1, M_S=0$ $(M_S=-1)$. As a result, the outgoing wave function is in the state $|10;11\rangle$ for one spin flip, and in the total spin state $|1-1;11\rangle$ after the two-spin-flip interaction. The Clebsch-Gordan coefficients for each process are given by $\sqrt{3/10}$ and $\sqrt{3/5}$, i.e., the spin part of the transition matrix contributing to the decay rate is a factor of $\sqrt{2}$ larger for the two-spin-flip process than for the one-spin-flip process. Moreover, the energy released in a one-spin-flip process is only half of the energy released in a two-spin-flip process. Therefore, we find that $p^{1SF}_{\alpha',\beta'} = \sqrt{2m\mu_e B}$, whereas $p^{2SF}_{\alpha',\beta'} = \sqrt{4m\mu_e B}$. We thus arrive at the convenient relation that $G^{2SF}(B) = 2G^{1SF}(2B)$ and it suffices to calculate only the one-spin-flip decay rate.

Performing a similar calculation as in the case of the exchange decay rates, the one-spin-flip decay rate becomes

$$
\begin{aligned}
G^{1SF}(B) = 2\pi^3\hbar^2 m \sqrt{2m\mu_e B} \left| \frac{\mu_0 \mu_e^2}{4\pi} \sqrt{\frac{4\pi}{5}} \right. \\
\times \left\langle \Psi^{(-)}_{211}(\mathbf{r}) \left| \frac{Y_{21}(\hat{\mathbf{r}})}{r^3} \right| \Psi^{(+)}_{001}(\mathbf{r}) \right\rangle \\
\left. \times \langle 10;11| \Sigma^{ee}_{2,-1} |11;11\rangle \right|^2 \\
= \frac{12}{10} \sqrt{2m\mu_e B} \frac{m(\mu_0\mu_e^2)^2}{\pi\hbar^4} (r_{20})^2,
\end{aligned}
\tag{7}
$$

where

$$
(r_{20})^2 = \int_0^\infty dr \frac{\psi^{(-)}_{21}(r) \psi^{(+)}_{01}(r)}{r^3}
$$

is the radial electron-electron dipolar element. In Fig. 2 the one-spin-flip decay rate constant is shown as curve 2.

At this point it can be understood that the electron-electron dipolar interaction gives the largest contribution to the dipolar decay rates. Decay due to the electron-nucleon interaction occurs, for example, via the $|\{6,5\}_-\rangle \rightarrow |\{6,4\}_-\rangle$ channel. However, the corresponding decay rates are smaller by a factor of $(\mu_N/\mu_e)^2 \simeq 20 \times 10^{-6}$ and thus completely negligible. This also implies that a mixture of $|6\rangle$ and $|5\rangle$ atoms cannot achieve equilibrium in the spin degrees of freedom within the lifetime of the gas. This is completely analogous to the recent experiments with two condensates in different spin states performed by Myatt et al. [10].

Figure 2 shows that the lifetime of the gas is of the order of 1 s for a density $n_5 = n_6 \simeq 10^{12}$ cm^{-3} and a magnetic bias field of 5 T. Although this would provide ample time to perform an experiment, a much shorter lifetime may be adequate. For successful experiments we have to require not only that the time between thermalizing collisions is small compared to the lifetime of the gas, but also that the time scale for formation of the Cooper pairs obeys this condition. The latter is anticipated to be of $O(\hbar/k_B T_c)$ and therefore in our case much longer than the time between collisions. Nevertheless, for a density $n_5 = n_6 \simeq 10^{12}$ cm^{-3}, we have that $T_c \simeq 11$ nK and $\hbar/k_B T_c$ is only about 0.7 ms, where as a bias field of 0.2 T gives a lifetime of about 1 ms [16].

In the next subsection we consider the microscopic theory that describes the Fermi gas in the normal and the superfluid state. We apply only the BCS theory here. The influence of fluctuations [8] will be addressed elsewhere.

B. BCS transition

For the homogeneous case, and taking only two-body interactions between atoms in different hyperfine states into account, the gas is described by the Hamiltonian [15]

$$
\begin{aligned}
H = \sum_{\alpha=\uparrow,\downarrow} \left\{ \int d\mathbf{x} \, \psi^\dagger_\alpha(\mathbf{x}) \left(-\frac{\hbar^2\nabla^2}{2m} - \mu_\alpha \right) \psi_\alpha(\mathbf{x}) \right. \\
+ \frac{1}{2} \int d\mathbf{x} \int d\mathbf{x}' V_T(\mathbf{x}-\mathbf{x}') \\
\left. \times \psi^\dagger_\alpha(\mathbf{x}) \psi^\dagger_{-\alpha}(\mathbf{x}') \psi_{-\alpha}(\mathbf{x}') \psi_\alpha(\mathbf{x}) \right\}.
\end{aligned}
\tag{8}
$$

In this expression, $\uparrow$ and $\downarrow$ refer again to the two hyperfine states involved. The field operators $\psi_\alpha(\mathbf{x})$ and $\psi^\dagger_\alpha(\mathbf{x})$ obey the usual Fermi anticommutation relations and denote the annihilation and creation of a fermion at position $\mathbf{x}$ in hyperfine state $|\alpha\rangle$ with chemical potential μ_α. The interparticle potential can be approximated by a local potential $V_T(\mathbf{x} - \mathbf{x}') \simeq V_0 \delta(\mathbf{x}-\mathbf{x}')$, where the constant V_0 is a measure of the strength of the interaction. We will return to the precise value of V_0 shortly, but it is in any case negative to account for the effectively attractive nature of the triplet interaction. The integration over $\mathbf{x}'$ in the Hamiltonian is then trivial. The next step in a mean-field treatment of the Hamiltonian in Eq. (8) is to develop the operator products $\psi^\dagger_\alpha \psi_\alpha$ and $\psi_\alpha \psi_{-\alpha}$ around their mean values by substituting

$$
\psi^\dagger_\alpha \psi_\alpha = \langle \psi^\dagger_\alpha \psi_\alpha \rangle + \delta \psi^\dagger_\alpha \psi_\alpha
$$

and

$$
\psi_{-\alpha}\psi_\alpha = \langle \psi_{-\alpha}\psi_\alpha \rangle + \delta\psi_{-\alpha}\psi_\alpha.
$$

To first order in the fluctuations, we are left with the effective mean-field Hamiltonian

$$H = \int d\vec{x} \left\{ \sum_{\alpha=\uparrow,\downarrow} \psi_\alpha^\dagger(\mathbf{x}) \left(-\frac{\hbar^2 \nabla^2}{2m} - \mu_\alpha' \right) \psi_\alpha(\mathbf{x}) \right.$$

$$+ \Delta_0 \psi_\uparrow^\dagger(\mathbf{x}) \psi_\downarrow^\dagger(\mathbf{x}) + \Delta_0^* \psi_\downarrow(\mathbf{x}) \psi_\uparrow(\mathbf{x}) - \frac{|\Delta_0|^2}{V_0}$$

$$\left. - \frac{4\pi a \hbar^2}{m} n_\downarrow n_\uparrow \right\}, \tag{9}$$

where $n_\alpha = \langle \psi_\alpha^\dagger(\mathbf{x}) \psi_\alpha(\mathbf{x}) \rangle$ is the equilibrium value of the density of atoms in state $|\alpha\rangle$ and equivalently $\Delta_0 = V_0 \langle \psi_\downarrow(\mathbf{x}) \psi_\uparrow(\mathbf{x}) \rangle$ is the equilibrium value of the BCS order parameter [16]. The chemical potential of each hyperfine state has now been renormalized to $\mu_\alpha' = \mu_\alpha - T^{2B} n_{-\alpha}$ to include, on the mean-field level, all two-body scattering processes with particles in state $|-\alpha\rangle$. The factor $T^{2B} = 4\pi a \hbar^2/m$ is the two-body scattering matrix and has been substituted for V_0 to incorporate correctly all two-body processes into the calculation. Note that the same substitution should not be performed in the expression for Δ_0 because all two-body interactions are already going to be included by the BCS treatment as we will see below [14]. Due to the non-equilibrium in the spin degrees of freedom, both chemical potentials $\mu_\downarrow'$ and $\mu_\uparrow'$ need not be equal and therefore the densities of atoms in the respective hyperfine level can be varied independently.

Substituting for the operator $\psi_\alpha^\dagger$ the expression

$$\psi_\alpha^\dagger(\mathbf{x}) = \frac{1}{\sqrt{V}} \sum_{\mathbf{k}} a_{\mathbf{k},\alpha}^\dagger e^{-i\mathbf{k}\cdot\mathbf{x}}, \tag{10}$$

where $a_{\mathbf{k},\alpha}^\dagger$ creates one particle in spin state $|\alpha\rangle$ with momentum $\hbar\mathbf{k}$, the Hamiltonian in Eq. (9) becomes

$$H = \sum_{\mathbf{k}} (a_{\mathbf{k},\uparrow}^\dagger a_{-\mathbf{k},\downarrow}) \begin{pmatrix} \epsilon_{\mathbf{k}} - \mu_\uparrow' & \Delta_0 \\ \Delta_0^* & -\epsilon_{\mathbf{k}} + \mu_\downarrow' \end{pmatrix} \begin{pmatrix} a_{\mathbf{k},\uparrow} \\ a_{-\mathbf{k},\downarrow}^\dagger \end{pmatrix} - \frac{|\Delta_0|^2}{V_0}$$

$$- n_\uparrow n_\downarrow T^{2B}, \tag{11}$$

where $\epsilon_{\mathbf{k}} = \hbar^2 k^2/2m$ is the free particle energy of a particle with momentum $\hbar\mathbf{k}$. The density of atoms in state $|\alpha\rangle$ is determined by

$$n_\alpha = \langle \psi_\alpha^\dagger \psi_\alpha \rangle = \frac{1}{V} \sum_{\mathbf{k}} \langle a_{\mathbf{k},\alpha}^\dagger a_{\mathbf{k},\alpha} \rangle. \tag{12}$$

Since the effective mean-field Hamiltonian in terms of the operators $a_{\mathbf{k},\alpha}^\dagger$ and $a_{\mathbf{k},\alpha}$ is nondiagonal, one cannot directly calculate the expectation value $\langle a_{\mathbf{k},\alpha}^\dagger a_{\mathbf{k},\alpha} \rangle$.

This is, as usual, resolved by first applying a Bogoliubov transformation according to [16]

$$a_{\mathbf{k},\uparrow} = u_{\mathbf{k}} b_{\mathbf{k},\uparrow} + v_{\mathbf{k}}^* b_{-\mathbf{k},\downarrow}^\dagger, \tag{13a}$$

$$a_{-\mathbf{k},\downarrow}^\dagger = -v_{\mathbf{k}} b_{\mathbf{k},\uparrow} + u_{\mathbf{k}}^* b_{-\mathbf{k},\downarrow}^\dagger \tag{13b}$$

to diagonalize the Hamiltonian in Eq. (11). After performing this unitary transformation, we require that the Hamiltonian

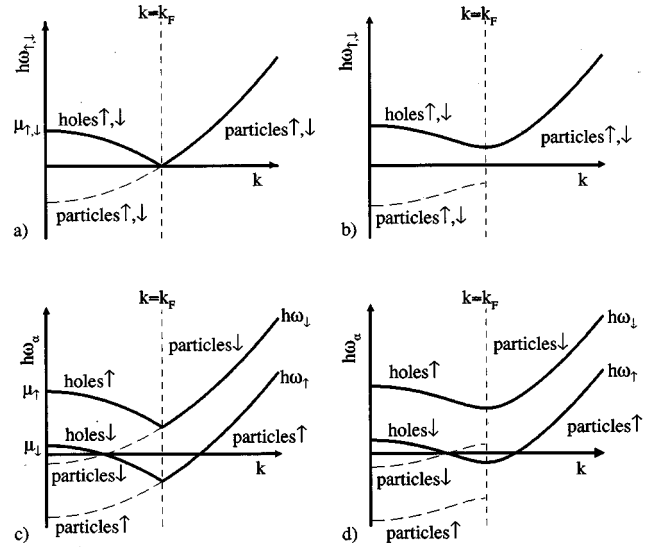

FIG. 3. Bogoliubov dispersion $\hbar \omega_{\mathbf{k},\alpha}$ for (a) $n_\uparrow = n_\downarrow$ and $\Delta_0 = 0$; (b) $n_\uparrow = n_\downarrow$ and $\Delta_0 \neq 0$, (c) $n_\uparrow > n_\downarrow$ and $\Delta_0 = 0$, and (d) $n_\uparrow > n_\downarrow$ and $\Delta_0 \neq 0$. The thin dashed lines indicate the particle dispersions below the Fermi level ϵ_F.

in terms of the new quasiparticle operators $b_{\mathbf{k},\uparrow}$ and $b_{-\mathbf{k},\downarrow}^\dagger$ has only diagonal elements and furthermore that these operators again obey the usual anticommutation relations for annihilation and creation operators. This determines the values of the yet unknown and in principle complex constants $u_{\mathbf{k}}$ and $v_{\mathbf{k}}$. The latter constraint requires that the constants $u_{\mathbf{k}}$ and $v_{\mathbf{k}}$ must satisfy the relations $|u_{\mathbf{k}}|^2 + |v_{\mathbf{k}}|^2 = 1$ and the requirement of diagonality of the Hamiltonian after the transformation leads to the condition $|u_{\mathbf{k}}|^2 = \frac{1}{2}(1 + \xi_{\mathbf{k}}/\sqrt{\xi_{\mathbf{k}}^2 + |\Delta_0|^2})$, introducing $\xi_{\mathbf{k}} = \epsilon_{\mathbf{k}} - \epsilon_F$, i.e., the free particle energy relative to the average Fermi level $\epsilon_F = (\mu_\uparrow' + \mu_\downarrow')/2$.

The eigenvalues corresponding to the Bogoliubov quasiparticles are then given by

$$\hbar \omega_{\mathbf{k},\alpha} = -m_\alpha \delta \epsilon_F + \sqrt{\xi_{\mathbf{k}}^2 + |\Delta_0|^2}, \tag{14}$$

where $m_\alpha = \pm 1/2$ for $\alpha = \uparrow, \downarrow$, respectively. Furthermore, $\delta \epsilon_F = \mu_\uparrow' - \mu_\downarrow'$ is the difference in Fermi levels of the two hyperfine states. The dispersion relations of Eq. (14) are depicted in Fig. 3 for equal [Figs. 3(a) and 3(b)] and unequal densities [Figs. 3(c) and 3(d)] with both zero [Figs. 3(a) and 3(c)] and nonzero Δ_0 [Figs. 3(b) and 3(d)], respectively [19].

Note that when the densities in both spin states are equal (corresponding to $\delta \epsilon_F = 0$), the dispersion relation reduces to the usual Bogoliubov dispersion $\hbar \omega_{\mathbf{k}} = \sqrt{\xi_{\mathbf{k}}^2 + |\Delta_0|^2}$ describing particles above the Fermi level, i.e., $\epsilon_{\mathbf{k}} > \epsilon_F$, and holes (for which the dispersion is given by minus the particle dispersion) below ϵ_F. It is clear that the Bogoliubov transformation couples particles in state $|\alpha\rangle$ with holes in state $|-\alpha\rangle$ [see, for example, Fig. 3(d)] and that for unequal densities the dispersion relations are shifted with a constant $\pm \delta \epsilon_F/2$ such that there appear two separate branches in the excitation spectrum of the Bogoliubov quasiparticles as shown in Figs. 3(c) and 3(d). For $n_\uparrow > n_\downarrow$, the negative sign of $\hbar \omega_{\mathbf{k},\uparrow}$ around the Fermi level ϵ_F indicates that the energy states are partially filled with spin-down holes below ϵ_F and with spin-up electrons in a small region above the Fermi

level. Therefore, the lower branch is *gapless* when $\Delta_0 < \delta\epsilon_F/2$, whereas the upper one always has a gap, even at $\Delta_0 = 0$. The case of unequal densities is thus analogous to a gapless superconductor.

By plugging the transformation Eq. (13) into Eq. (12), it is easily verified that the densities satisfy

$$n_\alpha = \frac{1}{V}\sum_{\mathbf{k}} \{|u_{\mathbf{k}}|^2 N(\hbar\omega_{\mathbf{k},\alpha}) + |v_{\mathbf{k}}|^2 [1 - N(\hbar\omega_{\mathbf{k},-\alpha})]\}, \tag{15}$$

where $N(\hbar\omega_{\mathbf{k},\alpha}) = 1/(\exp[\beta\hbar\omega_{\mathbf{k},\alpha}] + 1) = \langle b_{\mathbf{k},\alpha}^\dagger b_{\mathbf{k},\alpha}\rangle$ is the Fermi distribution for the Bogoliubov quasiparticles and $\beta = 1/k_B T$. For fixed n_α, Eq. (15) determines the chemical potentials μ'_α of the particles in state $|\alpha\rangle$.

Subsequently, the equilibrium value of the BCS order parameter is calculated from $\Delta_0 = V_0\langle\psi_\downarrow(\mathbf{x})\psi_\uparrow(\mathbf{x})\rangle$. Substituting Eqs. (10) and (13) for $\psi_{\uparrow,\downarrow}(\mathbf{x})$, this leads to the BCS "gap equation"

$$\frac{1}{V}\sum_{\mathbf{k}} \frac{1 - N(\hbar\omega_{\mathbf{k},\uparrow}) - N(\hbar\omega_{\mathbf{k},\downarrow})}{2\sqrt{\xi_{\mathbf{k}}^2 + |\Delta_0|^2}} = -\frac{1}{V_0}. \tag{16}$$

This equation has an ultraviolet divergence as a consequence of the fact that we made the assumption that the interparticle interaction is local, i.e., momentum independent. However, from the Lippmann-Schwinger equation for the two-body scattering matrix [20]

$$\frac{1}{T^{2B}} = \frac{1}{V_0} + \frac{1}{V}\sum_{\mathbf{k}} \frac{1}{2\xi_{\mathbf{k}}}, \tag{17}$$

we find that this divergence is canceled by a renormalization of $1/V_0$ to $1/T^{2B}$ [17] and the gap equation becomes

$$\frac{1}{V}\sum_{\mathbf{k}} \left\{ \frac{1 - N(\hbar\omega_{\mathbf{k},\uparrow}) - N(\hbar\omega_{\mathbf{k},\downarrow})}{2\sqrt{\xi_{\mathbf{k}}^2 + |\Delta_0|^2}} - \frac{1}{2\xi_{\mathbf{k}}} \right\} = -\frac{1}{T^{2B}}. \tag{18}$$

Eliminating from this equation both chemical potentials μ'_α by means of Eq. (15) and equating Δ_0 to zero, one finds the critical temperature T_c as a function of both hyperfine densities in the gas. If the hyperfine densities are taken to be equal, the critical temperature can be calculated analytically [21], resulting in

$$T_c \simeq \frac{8\epsilon_F}{k_B\pi} e^{\gamma-2}\exp\left\{-\frac{\pi}{2k_F|a|}\right\}, \tag{19}$$

where $\gamma = 0.5772$ is Euler's constant and $k_F = \sqrt{2m\epsilon_F}/\hbar$ is again the wave vector corresponding to the Fermi energy ϵ_F. Including fluctuations changes only the prefactor of Eq. (19) [8]. Although this is expected to lower the critical temperature somewhat, the exponential dependence of T_c on the scattering length is most important for our purposes. Since taking fluctuations into account self-consistently is rather difficult, in particular in the inhomogeneous case, we will return to the effect of fluctuations on the transition to a superfluid state elsewhere and consider here only the mean-field theory, which is also known as the many-body T-matrix theory.
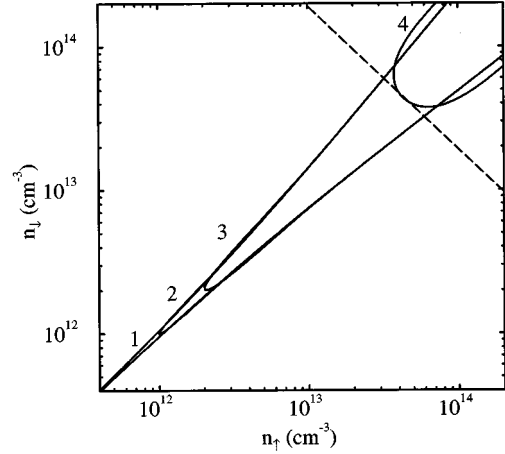

FIG. 4. Contours of the critical temperature as a function of the hyperfine densities $n_\uparrow$ and $n_\downarrow$ for (1) $T = 0.01$ nK, (2) $T = 11$ nK, (3) $T = 37$ nK, and (4) $T = 1725$ nK. The dashed line is the spinodal line.

As mentioned previously, the densities of particles, and hence the chemical potentials, need not be equal in both spinstates. In Fig. 4 we plot several contour plots of the critical temperature for the homogeneous gas in the $n_\uparrow$-$n_\downarrow$ plane. As can be seen from this figure, the most favorable situation is that, given a certain total density of atoms, both hyperfine states are equally occupied because this gives rise to the highest critical temperature. When the two hyperfine states are not equally occupied, it can be shown that there is a nonzero critical temperature only when the spin "polarization" $|n_\uparrow - n_\downarrow|/(n_\uparrow + n_\downarrow) < 3k_B T_c/2\epsilon_F$. Also, for fixed average Fermi level ϵ_F and increasing difference $\delta\epsilon_F$, the critical temperature decreases and there is no transition at all when $\delta\epsilon_F \gtrsim k_B T_c(0)$, with $T_c(0)$ the critical temperature when $\delta\epsilon_F = 0$ [4]. This behavior is similar to what occurs in superconductors placed in a magnetic field and can be understood physically from the fact that the formation of Cooper pairs spreads the occupation of energy levels only over an energy interval of order $\Delta_0 \simeq k_B T_c$ around the respective Fermi levels $\mu'_\uparrow$ and $\mu'_\downarrow$. Moreover, pairing between atoms at the average Fermi energy can only take place if there exists an overlap between the Fermi distributions of the two spin states in this region of momentum space. This indeed shows that $\delta\epsilon_F$ must be smaller than about $k_B T_c(0)$.

The dashed line in Fig. 4 is the spinodal line, above which the gas becomes mechanically unstable. We will return to this issue in the next subsection.

C. Mechanical stability of a two-component Fermi gas

As already pointed out in Ref. [4], an important requirement for a BCS transition to occur is that the system is mechanically stable against density fluctuations. The negative s-wave scattering length induces an effectively attractive interatomic potential, so if the density of particles becomes too large, the system can collapse to a fluid or solid state before the systems becomes superfluid in the (metastable) gaseous phase. In general, for mechanical stability of the gas at the critical temperature, we must require that the velocities of the two sound modes in the normal state of the gas are

real. These velocities can be calculated from the free-energy density f of the gas. Since the temperatures of interest are so low that $k_B T \ll \epsilon_F$, we can consider the zero-temperature limit, in which the free-energy density amounts to the average energy density $f = \langle E \rangle / V$. We thus have

$$f = f_0 + f_{int} \equiv \frac{3}{10} (6\pi^2)^{2/3} (n_\uparrow^{5/3} + n_\downarrow^{5/3}) \frac{\hbar^2}{m} + n_\uparrow n_\downarrow T^{2B},$$

(20)

where f_0 is the ideal gas free-energy density of the particles in each hyperfine state at $T = 0$ and f_{int} is the free-energy density that arises due to interactions between particles in both spin states. The corresponding sound velocities squared are determined by the eigenvalues of the matrix

$$\begin{pmatrix} \dfrac{\partial^2 f}{\partial n_\uparrow \partial n_\uparrow} & \dfrac{\partial^2 f}{\partial n_\uparrow \partial n_\downarrow} \\ \dfrac{\partial^2 f}{\partial n_\downarrow \partial n_\uparrow} & \dfrac{\partial^2 f}{\partial n_\downarrow \partial n_\downarrow} \end{pmatrix},$$

leading to the condition that $n_\uparrow n_\downarrow a^6 \leq (\pi/48)^2$. The line in the $n_\uparrow$-$n_\downarrow$ plane, where the equality holds, is called the spinodal line, and for the homogeneous ^{6}Li gas it is plotted as the dashed line in Fig. 4.

Notice, however, that a spin-polarized Fermi gas becomes unstable at densities above the spinodal line, irrespective of the sign of the scattering length a. Therefore, the question arise as to what exactly happens at densities above the spinodal line and whether there is a difference in the behavior for positive or negative s-wave scattering length. First of all, notice that the matrix $\partial^2 f / \partial n_\alpha \partial n_\beta$ has an eigenvalue $\lambda = 0$ at the spinodal point. The corresponding eigenvector $\hat{\mathbf{e}}_0$ points in the unstable direction of the phase space. For equal densities of the two hyperfine states, it is straightforward to calculate that $\hat{\mathbf{e}}_0 = 1/\sqrt{2}(\mp 1, 1)$, where the upper and lower signs refer to positive and negative scattering lengths a, respectively. We therefore conclude that for a negative s-wave scattering length, the gas collapses to a dense phase (probably a solid), whereas for positive a it phase separates into two dilute gaseous phases with opposite ''magnetization.'' Since the second situation might be of interest for future experiments with other fermionic atoms than ^{6}Li, we consider now for a moment also the $a > 0$ case.

1. The a > 0 case

To analyze the stability at positive a, we notice that the pressure of the gas at zero temperature is given by $p = -\partial \langle E \rangle / \partial V$. We thus find that

$$p = p_0 + p_{int} = \frac{1}{5} (6\pi^2)^{2/3} (n_\uparrow^{5/3} + n_\downarrow^{5/3}) \frac{\hbar^2}{m} + n_\uparrow n_\downarrow T^{2B}.$$

(21)

Introducing for future convenience dimensionless variables according to $x \equiv n_\uparrow a^3$, $y \equiv n_\downarrow a^3$, $M_{\uparrow,\downarrow} \equiv (2ma^2/\hbar^2)\mu_{\uparrow,\downarrow}$, $P \equiv a^3(2ma^2/\hbar^2)p$, and $F \equiv a^3(2ma^2/\hbar^2)f$, it follows from Eqs. (21) and (20) that
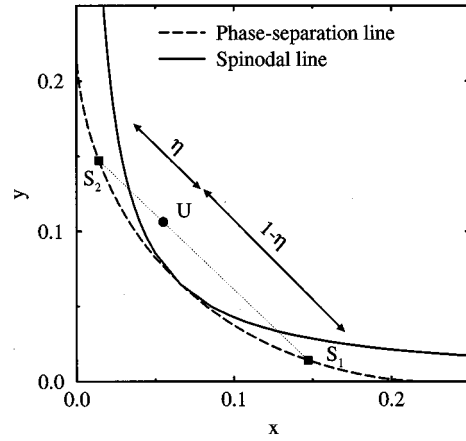

FIG. 5. Plot of the phase-separation line (dashed) as a function of the dimensionless densities $x = n_\uparrow a^3$ and $y = n_\downarrow a^3$, together with the spinodal line $xy = (\pi/48)^2$, above which the gas phase separates to the dashed line. As an example, the unstable phase U separates to the stable phases S_1 and S_2, with volume fractions $V_1 = \eta V$ and $V_2 = (1 - \eta)V$, respectively. Note that in the regions between the phase-separation line and the spinodal line, the gas is metastable.

$$P(x, y) = \frac{2}{5} (6\pi^2)^{2/3} (x^{5/3} + y^{5/3}) + 8\pi xy,$$

(22)

$$F(x, y) = \frac{3}{5} (6\pi^2)^{2/3} (x^{5/3} + y^{5/3}) + 8\pi xy,$$

(23)

$$M_\uparrow(x, y) = (6\pi^2)^{2/3} x^{2/3} + 8\pi y,$$

(24)

$$M_\downarrow(x, y) = (6\pi^2)^{2/3} y^{2/3} + 8\pi x,$$

(25)

where we used that $\mu_{\uparrow,\downarrow} = \partial f / \partial n_{\uparrow,\downarrow}$. Notice that these equations are symmetric under the exchange of the variables x and y or rather the indices $\uparrow$ and $\downarrow$.

The condition that must be fulfilled for a phase separation is that an unstable phase U separates into two distinct phases S_1 and S_2 in the stable region of the phase space in such a way that both the pressure and the chemical potential in the two stable phases are equal. Since in our case we are dealing with a gas consisting of two constituents, we require that both chemical potentials $\mu_\uparrow$ and $\mu_\downarrow$ must be equal in the two stable phases; otherwise particles would still prefer one phase above the other and there would be no equilibrium. A third condition that must hold is that the total number of particles in each spin state must be conserved. In Fig. 5 we show the spinodal line in terms of the dimensionless variables x, y, i.e., $xy = (\pi/48)^2$. Furthermore, we plotted an unstable point U, which separates into points $S_1 = (x_1, y_1)$ and $S_2 = (x_2, y_2)$ in the stable regime of phase space. Next we will deduce the exact position of these points S_1 and S_2 from the above-mentioned conditions on the phase separation.

From the condition on the pressure and the symmetry of Eq. (22) it follows that $P_{S_1} = P(x_1, y_1) = P_{S_2} = P(x_2, y_2)$ is satisfied if $x_1 = y_2$ and $x_2 = y_1$. In other words, the separation points S_1 and S_2 lie symmetric in the $n_\uparrow$-$n_\downarrow$ plane. The condition on the chemical potentials, i.e., $M_{\uparrow,\downarrow}(x_1, y_1) = M_{\uparrow,\downarrow}(x_2, y_2)$, now determines the exact position of the points $S_1 = (x_1, y_1)$ and $S_2 = (x_2, y_2)$. From the symmetry of

Eqs. (24) and (25) we see that $M_\uparrow(x_1,y_1)=M_\downarrow(y_1,x_1)$ $=M_\downarrow(x_2,y_2)$, so $M_\uparrow(x_i,y_i)=M_\downarrow(x_i,y_i)$ in each individual separation point $S_i, i=1,2$. This shows that, in practice, we are looking for intersections of the curves $M_\uparrow(x,y)=M_\downarrow(x,y)=M$. Again from symmetry, it is immediately clear that there is always a point of intersection of the two curves somewhere on the line $x=y$, but for certain values of M there can be two additional points of intersection, which are plotted as the dashed line in Fig. 5. This line is the phase-separation line. As we will prove later on, it coincides with the spinodal line at $x=y=\pi/48$ and lies below the spinodal line, in the stable region of phase space, elsewhere.

The third condition requiring conservation of the total number of particles in each spin state determines the volume fractions V_1/V and V_2/V of the two phases. For an unstable homogeneous system of volume V and with $N_\uparrow=n_\uparrow^U V$ and $N_\downarrow=n_\downarrow^U V$ particles in the two hyperfine states, we have that after the phase separation

$$N_\uparrow=n_\uparrow^{S_1}V_1+n_\uparrow^{S_2}V_2,$$

$$N_\downarrow=n_\downarrow^{S_1}V_1+n_\downarrow^{S_2}V_2.$$

Of course, the total density is also constant so we have $n_{total}=n_\uparrow^U+n_\downarrow^U=n_\uparrow^{S_1}+n_\downarrow^{S_1}=n_\uparrow^{S_2}+n_\downarrow^{S_2}$, which means that the points U, S_1, and S_2 must lie on a straight line given by $n_\uparrow+n_\downarrow=n_{total}$, as indicated for the points U, S_1, and S_2 by the dotted line in Fig. 5. Defining now $\beta^U=n_\uparrow^U/n_{total}$, $\beta^S=n_\downarrow^{S_1}/n_{total}=n_\uparrow^{S_2}/n_{total}$, and $\eta=(\beta^U-\beta^S)/(1-2\beta^S)$, we find after a little algebra that $V_1=\eta V$ and $V_2=(1-\eta)V$. So the phase separation is such that for arbitrary position of the point U on the unstable part of the dotted line in Fig. 5 the system separates into the same two stable points S_1 and S_2; the exact position of U determines only the volume fractions of the stable phases. The phase points S_1 and S_2 have the same total density but differ in "spin magnetization" by an amount $|n_\uparrow^{S_1}-n_\downarrow^{S_1}|$. Therefore, the phase separation corresponds to a spin decomposition that is driven by the fact that at sufficiently high densities the loss in interaction energy between the two species compensates for the gain in kinetic energy due to the Pauli exclusion principle.

To gain even more understanding in this phase separation and to distinguish later on the situation with negative a from the case with positive a, we consider the dimensionless free energy in Eq. (23) more closely. It is clear from Fig. 5 that the phase separation takes place on lines $x+y=$ const. Therefore, we introduce new variables n and z such that

$$x=n-z,$$

$$y=n+z,$$

i.e., the n axis lies along the line $x=y$ in Fig. 5 and the z axis lies along the line $y=-x$. Lines of constant $x+y$ therefore have a constant n (density) and run parallel to the z axis. The dimensionless free energy $F(x,y)$ in terms of these new variables now becomes

$$F(n,z)=\frac{3}{5}(6\pi^2)^{3/2}[(n-z)^{5/3}+(n+z)^{5/3}]+8\pi(n^2-z^2).$$
$$(26)$$

Note that, since the original variables x and y must be positive, also $n\geq0$, and for given n, we have $-n\leq z\leq+n$. Taking the derivative of $F(n,z)$ with respect to z at constant n, it is found that

$$\frac{\partial F}{\partial z}=(6\pi^2)^{2/3}[-(n-z)^{2/3}+(n+z)^{2/3}]-16\pi z,$$

which is zero at $z=0$ for all values of n. Hence there is always an extremum in the free energy $F(n,z)$ at the line $z=0$. To see whether this is a minimum or a maximum, we have to analyze the second derivative

$$\left.\frac{\partial^2 F}{\partial z^2}\right|_{z=0}=\frac{2}{3}(6\pi^2)^{2/3}\left[\frac{2}{n^{1/3}}\right]-16\pi,$$

which is positive for $n<n_{sp}=\pi/48$, zero at $n=n_{sp}$, and negative for $n>n_{sp}$. So the minimum in the free energy $F(n,z)$ at constant n and $z=0$ changes into a maximum at $n=n_{sp}$, which exactly coincides with the spinodal point at $x=y$. This behavior is shown in Fig. 6, where we plot $F(n,z)$ for (a) $n<n_{sp}$, (b) $n=n_{sp}$, and (c) and (d) $n>n_{sp}$, as a function of z.

From Fig. 6 we see that the maximum at $z=0$ for fixed $n>n_{sp}$ is flanked by two minima in the free energy, which move outward in the $\pm z$ directions for increasing n. Moreover, for $n=n_c=9\pi/256$ the minima just appear at $z=\pm n$, i.e., at the y axis in $y=9\pi/128$ and at the x axis in $x=9\pi/128$, respectively, in the original dimensionless density variables x and y. The important point is now that these two minima in the free energy $F(n,z)$ for fixed n are, after transforming back to x-y coordinates, precisely the stable separation points S_1 and S_2. Because of symmetry, they obey all conditions that we imposed on them. Furthermore, we notice that for $n>n_c$, or total density $n_{total}\geq9\pi/128a^3$, the spin separation is complete, i.e., one part of the volume is occupied with atoms only in the hyperfine level $|\uparrow\rangle$; the rest of the volume contains atoms only in state $|\downarrow\rangle$. The densities of both phases is in this case evidently $n_\uparrow^{S_1}=n_\downarrow^{S_2}=n_{total}$.

2. The $a<0$ case

We now consider the case where the scattering length $a<0$, as is the case for the ^{6}Li system. Introducing again dimensionless variables according to $x=n_\uparrow|a|^3$ and $y=n_\downarrow|a|^3$ and after the substitutions $x=n-z$ and $y=n+z$, respectively, the dimensionless free energy is readily seen to be

$$F(n,z)=\frac{3}{5}(6\pi^2)^{3/2}[(n-z)^{5/3}+(n+z)^{5/3}]-8\pi(n^2-z^2).$$
$$(27)$$

The first derivative of F in the z direction is given by

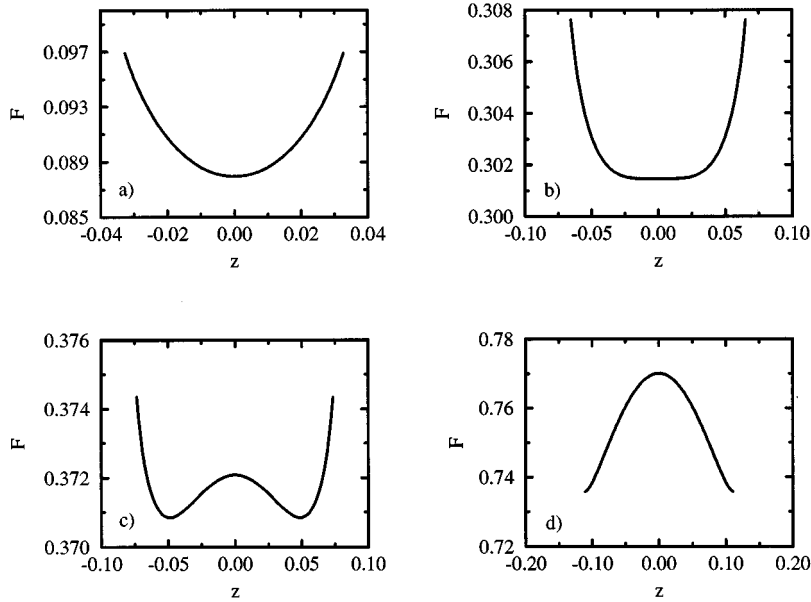$$\frac{\partial F}{\partial z}=(6\pi^2)^{3/2}[-(n-z)^{2/3}+(n+z)^{2/3}]+16\pi z,$$

FIG. 6. Plots of the dimensionless free energy $F(n,z)$ as a function of $z=(y-x)/2$, for (a) $n=\pi/96 < n_{sp}$, (b) $n=\pi/48=n_{sp}$, (c) $n_{sp} < n=6\pi/256 < n_c$, and (d) $n=9\pi/256=n_c$.

which is always zero at $z=0$. The second derivative with respect to the variable z at $z=0$ is given by

$$\frac{\partial^2 F}{\partial z^2} = \frac{2}{3}(6\pi^2)^{2/3}\left[\frac{2}{n^{1/3}}\right]+16\pi,$$

which is for all allowed values of n larger than zero. Therefore we conclude that there indeed can be no phase separation in the z direction along the lines $n=$const as was the case for positive a.

Instead, the phase separation in the unstable region of phase space above the spinodal line takes place in the n direction. This can be shown by considering the second derivative of F with respect to n, i.e.,

$$\frac{\partial^2 F}{\partial n^2} = \frac{2}{3}(6\pi^2)^{2/3}\left[\frac{1}{(n-z)^{1/3}}+\frac{1}{(n+z)^{1/3}}\right]-16\pi,$$

which at $z=0$ or $x=y$ becomes zero exactly at $n=n_{sp}=\pi/48$. The fact that the second derivative of the free energy is zero at some point signals an instability in that direction (in the $a>0$ case, the second derivative of F with respect to z just became zero at $n=n_{sp}$). So we find that in the case of negative scattering length, the unstable point U in phase space will separate into a phase S_1 with lower total particle density and a phase S_2 with higher total particle density or, in other words, to a gaseous and a dense (solid) state. However, we do not have an appropriate theory that can also describe the dense phase. Therefore, we do not consider this kind of phase separation, which is very common in gases and liquids, further here.

III. INHOMOGENEOUS FERMI GAS

A. Local-density approximation

Until now we considered only a homogeneous gas of spin-polarized atomic ^{6}Li. In reality, however, experiments with ultracold atomic gases are performed by trapping and evaporatively cooling the gas in an external potential that generally can be modeled by an isotropic harmonic oscillator $V(\mathbf{r})=\frac{1}{2}m\omega^2\mathbf{r}^2$, where ω is the trapping frequency. An exact calculation of the (inhomogeneous) density of the gas by calculating all eigenstates of the trapping potential is very elaborate but has nevertheless been performed for the bosonic isotopes ^{7}Li [22,23] and ^{87}Rb [24]. Fortunately, in the fermionic system it is a good approximation to make use of the local-density approximation, which treats the system as being locally homogeneous. This requires in the first place that the correlation length $\xi=O(1/k_F)$ is much shorter than the length scale $l=\sqrt{\hbar/m\omega}$ over which the densities change. This condition is equal to the condition that the level spacing $\hbar\omega$ of the trapping potential is much smaller than the Fermi energy. Second, below the critical temperature, the size of the Cooper pairs must be smaller than l or the trapping potential would influence the wave function of the Cooper pairs. This size is essentially temperature independent and of $O(\hbar v_F/\pi\Delta_0(0))$, where $\Delta_0(0)$ is the zero-temperature value of the BCS order parameter and $v_F=\hbar k_F/m$ the Fermi velocity corresponding to ϵ_F. Of course, the local-density approximation always breaks down at the edge of the gas cloud where the density vanishes and the effective Fermi energy becomes zero, and also at the critical temperature where the correlation length ξ diverges. So at a nonzero temperature below T_c there are two spatial regions where the local-density approximation is not valid, i.e., around the position where the local BCS order parameter vanishes and around the position where the local Fermi energy vanishes. However, these regions are so small that we do not expect any important changes in the functional behavior of physical properties at the crossover from outside to inside these regions. As a result, we believe that it is rather accurate to apply the local density approximation to calculate T_c [25,26].
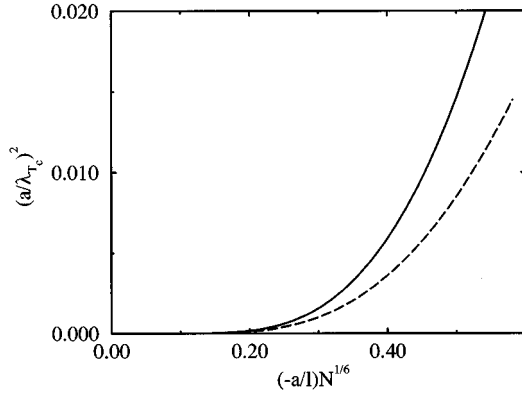
FIG. 7. Critical temperature as a function of the number of particles (solid line) when there are N particles present in both spin states. The dashed line represents the critical temperature for a gas whose density distribution is not altered by mean-field interactions.

In this approximation, the densities $n_\uparrow$ and $n_\downarrow$ of the two hyperfine states together with the gap Δ_0 can still be calculated by means of the equations derived in Sec. II B, with the understanding that now the effective chemical potentials, and consequently the densities and Δ_0, are spatially dependent through

$$\mu'_\alpha(\mathbf{r}) = \mu_\alpha - V(\mathbf{r}) - n_{-\alpha}(\mathbf{r})T^{2B}, \qquad (28)$$

where μ_α is the overall (constant) bare chemical potential of atoms in hyperfine state $|\alpha\rangle$. So, given T, $\mu_\downarrow$, and $\mu_\uparrow$ [or equivalently T, $N_\downarrow = \int d\mathbf{r}\, n_\downarrow(\mathbf{r})$, and $N_\uparrow = \int d\mathbf{r}\, n_\uparrow(\mathbf{r})$], one can determine the values of $n_\downarrow(\mathbf{r})$, $n_\uparrow(\mathbf{r})$, and $\Delta_0(\mathbf{r})$ self-consistently for every position $\mathbf{r}$ in space, as if the system were homogeneous. This procedure will be used in the next subsection to calculate the critical temperature of the spin-polarized gas as a function of the number of particles in the trap.

B. Critical temperature

The critical temperature T_c of the gas is such that at the center of the magnetic trap, where the density of the gas is highest, the energy gap $\Delta_0(\mathbf{0})$ just becomes nonzero for a given number of particles $N_\uparrow$ and $N_\downarrow$. First we will consider the case where $N_\uparrow = N_\downarrow = N$. In Fig. 7 the solid line shows the result of our calculation. The dashed line in this figure gives the critical temperature for the Fermi gas if one does not include the effects of the mean-field interaction in Eq. (28). In this approximation, the number of particles in each hyperfine state is, with a high degree of accuracy, given by the zero-temperature result $N_{\uparrow,\downarrow} = (\mu_{\uparrow,\downarrow}/\hbar\omega)^3/6$ and the density in the center of the trap is $n_{\uparrow,\downarrow}(\mathbf{0}) = (2m\mu_{\uparrow,\downarrow}/\hbar^2)^{3/2}/6\pi^2$, which is considerably smaller than in case that the mean-field interaction is taken into account. As a result, the critical temperature obtained in this manner is substantially lower for an equal number of particles. From an experimental point of view, it is therefore important to include interactions to obtain a reliable estimate for the critical temperature as a function of the number of trapped particles.

We found that, as is also the case for a Bose gas in a harmonic trap [24], the critical temperature, or rather the dimensionless parameter a/λ_{T_c}, is a universal function of

$N^{1/6}a/l$, with the thermal de Broglie wavelength $\lambda_T = \sqrt{2\pi\hbar^2/mk_BT}$ and $l = \sqrt{\hbar/m\omega}$. The solid line in Fig. 7 can be fitted numerically very well with the expression

$$\left(\frac{a}{\lambda_{T_c}}\right)^2 = 0.037\exp\left\{-1.214\frac{l}{|a|}N^{-1/6} + 2.990\frac{|a|}{l}N^{1/6}\right\}$$

for the whole range of parameters shown in Fig. 7.

The fact that the critical temperature is a universal function of the parameter $N^{1/6}a/l$ can be understood easily by rewriting the gap equation (18) at the critical temperature in the form

$$\frac{\sqrt{\pi}}{4}\frac{\lambda_{T_c}}{a} = \int_0^\infty dx\,\sqrt{x}$$

$$\times \frac{N(-\delta\epsilon_F + |x/\beta - \epsilon_F|) + N(\delta\epsilon_F + |x/\beta - \epsilon_F|)}{2|x - \beta\epsilon_F|},$$

where $N(x) = 1/(\exp[\beta x] + 1)$ is the Fermi distribution. This shows that at the critical temperature, a/λ_{T_c} is a function of $\delta\epsilon_F/k_BT_c$ and ϵ_F/k_BT_c only. Equivalently, from the density for each spin state given in Eq. (15) and the fact that at the critical temperature the densities in the center of the trap $n_\alpha(\mathbf{0})$ are critical, we find that

$$n_\alpha(\mathbf{0})\lambda_{T_c}^3 = F_\alpha\left[\frac{\delta\epsilon_F}{k_BT_c}, \frac{\epsilon_F}{k_BT_c}\right].$$

So the central density of each spin state times the thermal wavelength is also a function of the dimensionless parameters $\delta\epsilon_F/k_BT_c$ and ϵ_F/k_BT_c. Combining these two equations, it follows that a/λ_{T_c} is directly related to the densities in the center of the trap, i.e.,

$$\frac{a}{\lambda_{T_c}} = F[n_\uparrow(\mathbf{0})\lambda_{T_c}^3, n_\downarrow(\mathbf{0})\lambda_{T_c}^3]. \qquad (29)$$

To prove now that a/λ_{T_c} is a function of $N^{1/6}a/l$, it should be noticed that in general in the local-density approximation for $T \gtrsim T_c$

$$n_\alpha(\mathbf{r})\lambda_T^3 = f_{3/2}(\exp\{\beta[\mu_\alpha - n_{-\alpha}(\mathbf{r})T^{2B} - V(\mathbf{r})]\}), \quad (30)$$

where $f_{3/2}(z(\mathbf{r}))$ is the Fermi function originating from integration over momenta and analogous to the Bose function $g_{3/2}(z)$. Applying this equation at $\mathbf{r} = 0$ and $T = T_c$, we find that both chemical potentials are functions of a/λ_{T_c} and the central densities of both hyperfine states and obey

$$\frac{\mu_\alpha}{k_BT_c} = F'_\alpha\left[\frac{a}{\lambda_{T_c}}, n_\uparrow(\mathbf{0})\lambda_{T_c}^3, n_\downarrow(\mathbf{0})\lambda_{T_c}^3\right].$$

For a general value of $\mathbf{r}$, but still at $T = T_c$, we can apply the substitution

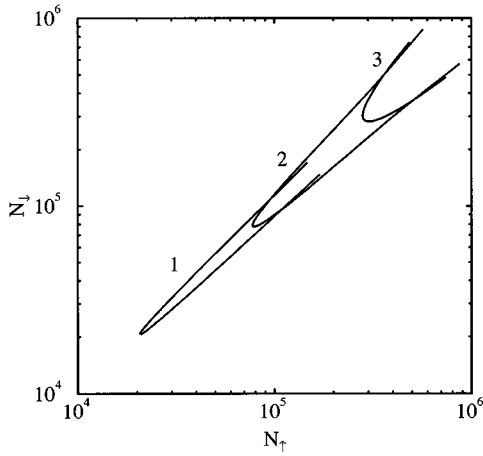$$y = \sqrt{\frac{m\omega^2}{2k_BT_c}}r \qquad (31)$$

FIG. 8. Critical temperature as a function of the number of ^{6}Li atoms in each hyperfine state. Curves 1–3 give the combinations $(N_\uparrow, N_\downarrow)$ corresponding to (1) $T_c = 3$ nK, (2) $T_c = 11$ nK, and (3) $T_c = 37$ nK. For equal number of particles in each hyperfine state, the density of particles in the center of the trap corresponds to (1) $n_{\uparrow,\downarrow}(\mathbf{0}) = 0.5 \times 10^{12}$ cm^{-3}, (2) 1×10^{12} cm^{-3}, and (3) 2×10^{12} cm^{-3}, respectively.

in Eq. (30), from which it follows immediately that for each hyperfine state

$$n_\alpha(\mathbf{r})\lambda_{T_c}^3 = F''_\alpha\left[\frac{a}{\lambda_{T_c}}, n_\uparrow(\mathbf{0})\lambda_{T_c}^3, n_\downarrow(\mathbf{0})\lambda_{T_c}^3, y^2\right].$$

To find the total number of particles in each hyperfine level, we then integrate this result over the spatial extent of the gas cloud, resulting in

$$
\begin{aligned}
N_\alpha &= 4\pi \int_0^\infty dr\, r^2 n_\alpha(r) = \frac{4\pi}{\lambda_{T_c}^3}\left(\frac{2k_B T_c}{m\omega^2}\right)^{3/2} \\
&\quad \times \int dy\left\{ y^2 F''_\alpha\left[\frac{a}{\lambda_{T_c}}, n_\uparrow(\mathbf{0})\lambda_{T_c}^3, n_\downarrow(\mathbf{0})\lambda_{T_c}^3, y^2\right]\right\} \\
&\equiv \left(\frac{l}{\lambda_{T_c}}\right)^6 F'''_\alpha\left[\frac{a}{\lambda_{T_c}}, n_\uparrow(\mathbf{0})\lambda_{T_c}^3, n_\downarrow(\mathbf{0})\lambda_{T_c}^3\right]. \quad (32)
\end{aligned}
$$

Multiplying Eq. (32) on both sides by $(a/l)^6$ and using the result of Eq. (29), it is proved that at the critical temperature

$$\frac{a}{\lambda_{T_c}} = F\left[N_\uparrow^{1/6}\frac{a}{l}, N_\downarrow^{1/6}\frac{a}{l}\right], \quad (33)$$

so that, when $\mu_\uparrow = \mu_\downarrow$ the dimensionless parameter a/λ_{T_c} is a universal function of $N^{1/6}a/l$.

The spinodal point in this case is given by $N^{1/6}a/l \simeq 0.66$ and is not included in Fig. 7 because for ^{6}Li trapped in a harmonic potential with frequency $\nu = \omega/2\pi = 144$ Hz, or $\hbar\omega/k_B \simeq 6.9$ nK, corresponding to the present experimental conditions of the experiment of Bradley *et al.* [2], spinodal decomposition only occurs with as many as 5.8×10^7 particles.

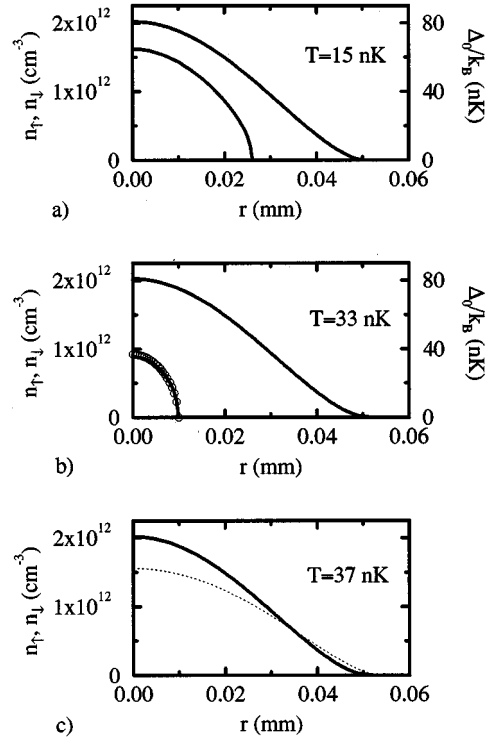For an unequal number of particles in each hyperfine state, we find a universal surface for a/λ_{T_c} as a function of

FIG. 9. Density distribution $n_\uparrow(\mathbf{r}) = n_\downarrow(\mathbf{r})$ and energy gap $\Delta_0(\mathbf{r})$ for a ^{6}Li atomic gas consisting of 2.865×10^5 atoms in each spin state at (a) $T = 15$ nK, (b) at $T = 33$ nK, slightly below T_c, and (c) at $T = T_c = 37$ nK. The left scale of each plot refers to the density and the right scale to the energy gap. The open circles in (b) represent Eq. (34) and the dotted line in (c) shows the density distribution for a gas with the same number of particles and at the same temperature, but with $a = 0$.

$N_\downarrow^{1/6}a/l$ and $N_\uparrow^{1/6}a/l$, as Eq. (33) shows. However, since we are in this paper mainly interested in trapping ^{6}Li atoms, we will calculate several contours of the critical temperature of such a gas trapped in an isotropic harmonic oscillator with $\nu = 144$ Hz. The results are plotted in Fig. 8. Again we see that given the total number of particles in the gas, the most favorable situation is the one with equal numbers of particles in each hyperfine state.

An important experimental question is how we could observe whether or not the gas is superfluid at a certain temperature. An immediate possibility that, in view of the results with the BEC experiments, comes to mind is to consider whether there is a change in the density profile at the critical temperature. In the next subsection we will therefore concentrate on the superfluid state of the gas and determine the density profiles and in addition the spatial dependence of the energy gap $\Delta_0(\mathbf{r})$.

C. Superfluid state

In Fig. 9 the density profile $n_\uparrow(\mathbf{r}) = n_\downarrow(\mathbf{r})$ and the energy gap $\Delta_0(\mathbf{r})$ are plotted for several temperatures below and at the critical temperature for a gas with $N_\uparrow = N_\downarrow = 2.865 \times 10^5$ particles in both hyperfine states. The dotted line in Fig. 9(c) shows the density distribution for a gas with the same number of particles, but with $a = 0$ instead of $a = -2160a_0$. It is clearly visible that the effect of the interaction on the density
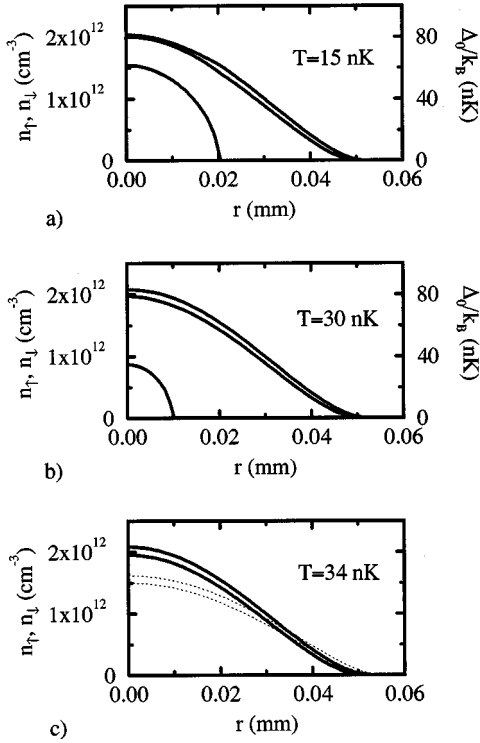
FIG. 10. Density distribution $n_\uparrow(\mathbf{r})$, $n_\downarrow(\mathbf{r})$, and energy gap $\Delta_0(\mathbf{r})$ for a ^{6}Li atomic gas with $N_\uparrow = 3.08 \times 10^5$ and $N_\downarrow = 2.65 \times 10^5$ below and at the critical temperature. (a) $T = 15$ nK, (b) at $T = 30$ nK, slightly below T_c, and (c) at $T = T_c = 34$ nK. The left scale of each plot refers to the density and the right scale to the energy gap. The dotted lines in (c) represent the density profiles for a noninteracting gas, with the same number of particles $N_\uparrow = 3.08 \times 10^5$ and $N_\downarrow = 2.65 \times 10^5$, respectively.

is rather large. Indeed, because of the attractive interactions, the particles are pulled to the center of the trap and the density is there considerably increased, which is good from an experimental point of view because it significantly increases the critical temperature.

Figure 10 is a similar plot, but now with unequal number of particles in each spin state: $N_\uparrow = 3.08 \times 10^5$ and $N_\downarrow = 2.65 \times 10^5$, so the total number of particles is the same as in the previous case. From Fig. 10(a) it can be seen that the presence of the order parameter tends to decrease the difference in densities of each hyperfine level. This can physically be understood from the fact that the most favorable condition for the formation of Cooper pairs is that both densities are equal.

The most important observation that we can make from both Figs. 9 and 10 is that there is almost no change in the density of the gas going from the normal to the superfluid phase. This also leads, as will be explained in more detail below, to the conclusion that a measurement of collective excitations will not give a good signature for the presence of a superfluid state [27]. A second observation is that from the BCS theory in superconductors [16], it is known that the order parameter Δ_0 close to the critical temperature vanishes as

$$\Delta_0(T) \simeq 1.74 \Delta_0(0) \sqrt{1 - T/T_c}, \qquad (34)$$

where $\Delta_0(0)$ is the zero-temperature value of Δ_0, which in turn is related to the critical temperature as

$$\Delta_0(0) \simeq 1.76 k_B T_c. \qquad (35)$$

For Fig. 9(a) it follows from Eq. (19) that the critical temperature corresponding to the density of the gas in the center of the trap is much larger than the temperature ($T = 15$ nK) itself. Hence the value of the order parameter approaches the zero-temperature limit in this case. Using that $T_c[n(\mathbf{0})] \simeq 37$ nK, one finds from Eq. (35) that $\Delta_0(0)/k_B = 65.1$ nK. Comparing this with $\Delta_0(\mathbf{r}=\mathbf{0})/k_B = 65.0$ nK, we find that there is indeed rather good agreement. Also, since the temperature in Fig. 9(b) is only slightly below the critical temperature, we can compare relation (34) with the values of $\Delta_0(\mathbf{r})$ in this figure. At each spatial position where $\Delta_0(\mathbf{r}) > 0$, we can, from the local value of the Fermi energy $\epsilon_F(\mathbf{r})$, extract the local critical temperature $T_c(\mathbf{r})$ from Eq. (19) and use Eq. (35) to compare $\Delta_0(T[\mathbf{r}])/k_B = 3.06 T_c(\mathbf{r}) \sqrt{1 - T/T_c(\mathbf{r})}$ [open circles in Fig. 9(b)] with $\Delta_0(\mathbf{r})$. Again, the agreement is very good.

Finally, we want to check that our local-density approximation is indeed valid under the conditions of interest. From Fig. 9 one finds that at $r = 0$, the value of $1/k_F l \simeq 0.06$ and, for example, at $r = 0.05$ mm, we find $1/k_F l \simeq 0.64$. Furthermore, from the zero-temperature value of Δ_0 in Eq. (35) we find that the size of the Cooper pairs relative to the trapping parameter l is about 0.58, so the local-density approximation starts to break down if we are far below the critical temperature. In that case a more accurate approach is required, at least for the relatively large trapping frequencies used here.

IV. DISCUSSION AND CONCLUSION

As mentioned above, an important experimental problem is the detection of the superfluid state. In contrast to the Bose-Einstein condensation experiments, there is no clear signature in the density distribution when the gas becomes superfluid, as shown in Sec. III C. Therefore, a measurement of the collective excitations, or density fluctuations, will not provide useful information on the presence of the superfluid phase as well. This can also be understood from the dissipationless (linear) hydrodynamic equations governing the density fluctuations in the system. Considering only the optimal situation of an equal number of particles $N_\uparrow = N_\downarrow$, these equations are given, for a gas trapped in an external potential $V(\mathbf{r})$, by

$$\frac{\partial n}{\partial t} + \boldsymbol{\nabla} \cdot \mathbf{j}^n = 0, \qquad (36a)$$

$$\frac{\partial \mathbf{j}^n}{\partial t} + \frac{1}{m}[\boldsymbol{\nabla} p + n \boldsymbol{\nabla} V(\mathbf{r})] = 0, \qquad (36b)$$

$$\frac{\partial \varepsilon}{\partial t} + \boldsymbol{\nabla} \cdot \mathbf{j}^\varepsilon = 0, \qquad (36c)$$

$$\frac{\partial \mathbf{v}_s}{\partial t} + \frac{1}{m} \boldsymbol{\nabla} \mu = 0, \qquad (36d)$$

where $n = n_n + n_s$ is the total density that consists of a normal and superfluid part, $\mathbf{j}^n = n_n\mathbf{v}_n + n_s\mathbf{v}_s$ is the density current with $\mathbf{v}_s$ ($\mathbf{v}_n$) the superfluid (normal) velocity, ε is the average energy density, $\mathbf{j}^\varepsilon = \mu\mathbf{j}^n + Ts\mathbf{v}_n$ is the energy current, and s is the entropy density [28,26]. Note that the same equations in fact also describe the collective modes of a trapped Bose-condensed gas [29,30].

To show that these hydrodynamic equations result in identical equations for the collective excitations in the normal and the superfluid phase, we first of all note that for the densities of interest the gas will be in the hydrodynamic limit, meaning that the time scales for the density fluctuations (which are of the order of the inverse trapping frequency) are much slower than the time between elastic collisions. In this hydrodynamic regime, density fluctuations and temperature fluctuations influence each other with a coupling proportional to $c_V - c_p$, where c_V (c_p) is the heat capacity per particle at constant volume (pressure). However, for the very low temperatures of interest, one can assume that the heat capacities of the gas satisfy $c_V \simeq c_p$. Indeed, for a homogeneous Fermi gas, one finds in the limit $T \downarrow 0$ that $(c_p - c_V)/C_v = O((k_B T/\epsilon_F)^2)$ and is thus very small. As a result, the density and temperature fluctuations are effectively uncoupled [27]. As a consequence, Eq. (36c), describing second sound, decouples from the other three equations and it suffices to consider only density fluctuations $n(\mathbf{r},t) = n_0(\mathbf{r}) + \delta n(\mathbf{r},t)$. Note also that if we have an unequal number of particles, i.e., $N_\uparrow \neq N_\downarrow$, the density fluctuations are coupled to fluctuations in the magnetization $n_\uparrow - n_\downarrow$ and we need to generalize these equations. For equal number of particles these ''spin waves'' decouple, however, as we have seen in Sec. II C.

In the normal phase, the Josephson relation Eq. (36d) must be dropped. Linearizing Eq. (36b), which is in fact just Newton's law, we arrive at

$$n_0(\mathbf{r})\frac{\partial \mathbf{v}(\mathbf{r},t)}{\partial t} = -\frac{1}{m}\boldsymbol{\nabla}\left(p[n_0(\mathbf{r})] + \frac{\partial p}{\partial n}\delta n(\mathbf{r},t)\right)$$
$$-\frac{1}{m}n_0(\mathbf{r})\boldsymbol{\nabla}V(\mathbf{r}) - \frac{1}{m}\delta n(\mathbf{r},t)\boldsymbol{\nabla}V(\mathbf{r})$$
$$= -\frac{1}{m}\boldsymbol{\nabla}\left(\frac{\partial p}{\partial n}\delta n(\mathbf{r},t)\right) - \frac{1}{m}\delta n(\mathbf{r},t)\boldsymbol{\nabla}V(\mathbf{r}),$$

where in the second line we used that in equilibrium

$$\boldsymbol{\nabla}p[n_0(\mathbf{r})] = -n_0(\mathbf{r})\boldsymbol{\nabla}V(\mathbf{r}) \tag{37}$$

and furthermore that the pressure p is a function of the density only at fixed temperature. This result, together with the continuity equation (36a), describes first sound in a trapped Fermi gas.

In the superfluid phase, first sound has $\mathbf{v}_s = \mathbf{v}_n$ and Eq. (36b) now becomes

$$n_0(\mathbf{r})\frac{\partial \mathbf{v}_s}{\partial t} = -\frac{1}{m}\boldsymbol{\nabla}\left(\frac{\partial p}{\partial n}\delta n(\mathbf{r},t)\right) - \frac{1}{m}\delta n(\mathbf{r},t)\boldsymbol{\nabla}V(\mathbf{r})$$
$$= -\frac{1}{m}\left(\boldsymbol{\nabla}\frac{\partial p}{\partial n} + \boldsymbol{\nabla}V(\mathbf{r})\right)\delta n(\mathbf{r},t) - \frac{1}{m}\frac{\partial p}{\partial n}\boldsymbol{\nabla}\delta n(\mathbf{r},t). \tag{38}$$

However, in the superfluid phase we also have the Josephson relation (36d) for the superfluid velocity. Using that the local chemical potential $\mu = \mu_0[n_0(\mathbf{r}) + \delta n(\mathbf{r},t)] + V(\mathbf{r})$, where μ_0 is the homogeneous chemical potential including the effects of interactions, and linearizing also this equation leads to

$$n_0(\mathbf{r})\frac{\partial \mathbf{v}_s}{\partial t} = -\frac{n_0(\mathbf{r})}{m}\boldsymbol{\nabla}\left(\mu_0[n_0(\mathbf{r})] + \frac{\partial \mu_0}{\partial n}\delta n(\mathbf{r},t) + V(\mathbf{r})\right)$$
$$= -\frac{n_0(\mathbf{r})}{m}\left(\delta n(\mathbf{r},t)\boldsymbol{\nabla}\frac{\partial \mu_0}{\partial n} + \frac{\partial \mu_0}{\partial n}\boldsymbol{\nabla}\delta n(\mathbf{r},t)\right) \tag{39}$$

because in equilibrium the chemical potential must satisfy

$$\mu_0[n_0(\mathbf{r})] + V(\mathbf{r}) = \text{const}. \tag{40}$$

Since in general

$$\frac{\partial p}{\partial n} = n_0\frac{\partial \mu_0}{\partial n}, \tag{41}$$

the second term on the right-hand side of Eq. (39) equals the last term on the right-hand side of Eq. (38). Moreover, the first term on the right-hand side of Eq. (39) can be rewritten with Eq. (41) as

$$\boldsymbol{\nabla}\frac{\partial \mu_0}{\partial n} = -\frac{\partial p}{\partial n}\frac{1}{n_0^2(\mathbf{r})}\boldsymbol{\nabla}n_0(\mathbf{r}) + \frac{1}{n_0(\mathbf{r})}\boldsymbol{\nabla}\frac{\partial p}{\partial n}$$
$$= -\frac{1}{n_0^2(\mathbf{r})}\boldsymbol{\nabla}p + \frac{1}{n_0(\mathbf{r})}\boldsymbol{\nabla}\frac{\partial p}{\partial n}$$
$$= \frac{1}{n_0(\mathbf{r})}\left(\boldsymbol{\nabla}\frac{\partial p}{\partial n} + \boldsymbol{\nabla}V(\mathbf{r})\right),$$

where we used again the equilibrium condition in Eq. (37). We thus find that below the critical temperature, the Josephson relation (36d) is identical to the momentum equation (36b). As in the normal phase, first sound can below T_c thus be described merely by Eqs. (36a) and (36b). In combination with the results that the density profiles in the normal and superfluid phase are almost equal, we conclude that the hydrodynamic equations that describe the density fluctuations are almost identical and therefore that there will be no significant difference in the collective excitation spectrum in the superfluid and normal phase, respectively. Consequently, other means of experimental detection must be investigated. Of course, this conclusion is based on experiments that couple directly to density fluctuations such as in Refs. [31,32]. If one can couple also to second sound one would of course observe an additional mode below T_c.

Another possible way to detect the superfluid state is by a measurement of the two-body decay rate of the gas. Note that, in our case, three-body recombination processes are strongly suppressed since we are dealing with fermions and only have two different hyperfine states occupied. Above the critical temperature, the two-body rate constants are essentially independent of T and the magnitude is depicted as a function of the applied magnetic field in Fig. 2. In analogy to the case of a Bose gas, where the presence of a condensate decreases the decay rate due to two-body processes by a factor of about 2 [33–35], we now analyze the change in the decay rate due to the presence of Cooper pairs in the Fermi gas below the critical temperature.

Using the correlator method from Ref. [33], it is found that the decay rate constant due to two-body processes is given by

$$G(T) = G(T_c)K^{(2)}(T), \tag{42}$$

where the correlator

$$K^{(2)}(T) = \frac{1}{n_\uparrow n_\downarrow}\langle \psi_\uparrow^\dagger(\mathbf{x})\psi_\downarrow^\dagger(\mathbf{x})\psi_\downarrow(\mathbf{x})\psi_\uparrow(\mathbf{x})\rangle \tag{43}$$

equals 1 above T_c, but increases due to the nonzero expectation value $\langle \psi_\uparrow(\mathbf{x})\psi_\downarrow(\mathbf{x})\rangle$ below the critical temperature. Indeed, using the transformations given by Eqs. (10) and (13), it is found that

$$K^{(2)}(T) = 1 + \frac{|\Delta_0|^2}{V_0^2 n_\uparrow n_\downarrow},$$

where Δ_0/V_0 is again given by the ultraviolet-diverging expression (16). The question now arises what we should use for V_0 in this expression. Clearly, the denominator V_0 should not be considered as the zero-momentum component of the triplet potential. Physically, this can be understood by the fact that this value of V_0 does not characterize the exact nonlocal two-body triplet potential in any way. It does not even reproduce the correct long-distance behavior for the scattered wave function. Therefore, a first guess would be to replace V_0 by T^{2B}, but since the s-wave scattering length in this case is much larger than the effective range r_V of the interaction $V_T(\mathbf{x})$, it is likely that the replacement of V_0 by T^{2B} underestimates the effect of the presence of the superfluid phase on the decay rates considerably.

Instead, from our procedure to remove the ultraviolet divergence in the gap equation, we see that V_0 should be chosen such that it satisfies the Lippmann-Schwinger equation

$$\frac{1}{T^{2B}} = \frac{1}{V_0} + \frac{1}{V}\sum_{|\mathbf{k}|\leqslant\Lambda}\frac{1}{2\xi_\mathbf{k}},$$

where a cutoff $\Lambda = O(1/r_V)$ is introduced. Solving this equation for V_0 and using that the Fermi energy $\epsilon_F \ll \hbar^2\Lambda^2/2m$, we find that

$$V_0 = T^{2B}\frac{1}{1 - \dfrac{2a\Lambda}{\pi}}. \tag{44}$$

Applying this result, we can now make an estimate of the effect of the presence of the superfluid phase. To simplify the calculation, we will calculate the effect at $T = 0$ for a homogeneous gas with $n_\uparrow = n_\downarrow = n$. We then have that $n = k_F^3/6\pi^2$. Moreover, from the BCS theory we know that the zero-temperature value of the order parameter $\Delta_0(0)$ is related to the critical temperature by $\Delta_0(0) = 1.76k_BT_c$. So

$$\frac{1}{n_\uparrow n_\downarrow}\frac{|\Delta_0|^2}{V_0^2} \simeq \frac{1}{n^2}\left(\left[1 - \frac{2a\Lambda}{\pi}\right]\frac{1.76k_BT_c}{\epsilon_F}\frac{3\pi n}{4k_Fa}\right)^2.$$

From the functional behavior of the triplet potential $V_T(\mathbf{x})$, we deduce that the range of the two-body interaction $r_V \simeq 100a_0$. Therefore, substituting $\Lambda \simeq (100a_0)^{-1}$ and $a = -2160a_0$, we find that in the case of ^{6}Li atoms $V_0 \simeq 0.07T^{2B}$. Note that, as expected, the Fermi wave number k_F is much smaller than the cutoff value Λ: For a density $n_\uparrow = n_\downarrow = 10^{12}$ cm^{-3}, we have $\epsilon_F \simeq 6\times10^{-7}k_B$, resulting in $k_F \simeq (5\times10^3a_0)^{-1}$, which is indeed much smaller than the cutoff Λ. Using that $T_c = 11$ nK for $n = 10^{12}$ cm^{-3} (see Fig. 4), it turns out that $1 - 2a\Lambda/\pi \simeq 15$ and the correlator $K^{(2)}(0) \simeq 7$, which is much larger than its value above the critical temperature. Had we used T^{2B} instead of V_0, the change in the correlator would have been only of the order of 3%. Even though we do not expect that the corrections to the decay rates are as large as the above crude argument suggests, we do believe that it might be of the order unity and may be measurable. Of course, the cutoff dependence of V_0 should in some way drop out of the theory eventually, but for this a better theory is needed, which takes into account the precise details of the triplet potential and does not make use of a pseudopotential to replace it. Work along these lines is in progress because of the experimental importance to have a reliable estimate of the changes in the relaxation rate constants. Furthermore, note that the correlator $K^{(2)}(T)$ from Eq. (43) also appears in the expression of the average energy of the system [36]. A measurement of this quantity has been done for the case of Bose gases [37,38] and we believe that also in the case of fermions, a change in the average energy at the critical temperature can signal the presence of the superfluid phase.

In summary, we considered a gas of atomic ^{6}Li occupying two hyperfine states trapped in a magnetic field. Atoms in different hyperfine levels can interact via s-wave scattering. Using the most up-to-date triplet potential, we showed that the lifetime of such a gas with a density of 10^{12} cm^{-3} per hyperfine level is of the order of 1 s when a magnetic bias field of 5 T is applied. At this density the gas becomes superfluid at a temperature of about 11 nK. We also investigated the mechanical stability of a two-component Fermi gas and showed that if the two-particle interaction is repulsive, the gas is unstable for spin-density fluctuations, whereas in the case where the interatomic interaction is attractive, the gas is unstable against density fluctuations above the spinodal line.

Furthermore, we considered the superfluid state of atomic
^{6}Li, trapped in an isotropic harmonic-oscillator potential, in
the local-density approximation. We showed that the critical
temperature a/λ_{T_c} is a universal function of the quantities
$N_\uparrow^{1/6} a/l$ and $N_\downarrow^{1/6} a/l$. Below the critical temperature there is
almost no change in the density profile of the gas cloud.
Therefore, we suggest that the presence of the superfluid
state might be signaled by a change in the decay rates or a
change in the average energy at the critical temperature.

[1] M. H. Anderson, J. R. Ensher, M. R. Matthews, C. E. Wieman, and E. A. Cornell, Science **269**, 198 (1995).

[2] C. C. Bradley, C. A. Sackett, J. J. Tollett, and R. G. Hulet, Phys. Rev. Lett. **75**, 1687 (1995); C. C. Bradley, C. A. Sackett, and R. G. Hulet, *ibid.* **78**, 985 (1997).

[3] K. B. Davis, M. O. Mewes, M. R. Andrews, N. J. van Druten, D. S. Durfee, D. M. Kurn, and W. Ketterle, Phys. Rev. Lett. **75**, 3969 (1995).

[4] H. T. C. Stoof, M. Houbiers, C. A. Sackett, and R. G. Hulet, Phys. Rev. Lett. **76**, 10 (1996).

[5] E. R. I. Abraham, W. I. McAlexander, J. M. Gerton, R. G. Hulet, R. Côté, and A. Dalgarno, Phys. Rev. A **55**, R3299 (1997).

[6] A. J. Leggett, J. Phys. (France) IV **C7**, 19 (1980); J. M. V. A. Koelman, Ph.D. thesis, Eindhoven University of Technology, 1984 (unpublished).

[7] M. A. Baranov, Yu. Kagan, and M. Yu. Kagan, Pis'ma Zh. Éksp. Teor. Fiz. **64**, 273 (1996) [JETP Lett. **64**, 301 (1996)].

[8] L. P. Gor'kov and T. K. Melik-Barkhudarov, Zh. Éksp. Teor. Fiz. **40**, 1452 (1961) [Sov. Phys. JETP **13**, 1018 (1961)].

[9] P. Zoller (private communication).

[10] C. J. Myatt, E. A. Burt, R. W. Ghrist, E. A. Cornell, and C. E. Wieman, Phys. Rev. Lett. **78**, 586 (1997).

[11] A. G. K. Modawi and A. J. Leggett (unpublished).

[12] D. A. Butts and D. S. Rokhsar, Phys. Rev. A **55**, 4346 (1997).

[13] J. Oliva, Phys. Rev. B **39**, 4204 (1989).

[14] H. T. C. Stoof, M. Bijlsma, and M. Houbiers, NIST J. Res. **101**, 443 (1996), and references therein.

[15] H. T. C. Stoof, J. M. V. A. Koelman, and B. J. Verhaar, Phys. Rev. B **38**, 4688 (1988).

[16] Our distorted-wave Born approximation overestimates the spin-exchange rate constat at lower magnetic fields. Therefore, we have also performed a full coupled-channels calculation of this rate constant and find good agreement over the range of fields given in Fig. 2.

[17] See, for example, A. L. Fetter and J. D. Walecka, *Quantum Theory of Many Particle Systems* (McGraw-Hill, New York, 1971).

[18] P. de Gennes, *Superconductivity of Metals and Alloys*

(Addison-Wesley, New York, 1966).

[19] M. Houbiers and H. T. C. Stoof, Czech. J. Phys. **46**, 551 (1996).

[20] See, for example, W. Glöckle, *The Quantum Mechanical Few-Body Problem* (Springer, Berlin, 1983).

[21] C. A. R. Sá de Melo, M. Randeria, and J. R. Engelbrecht, Phys. Rev. Lett. **71**, 3202 (1993).

[22] M. Houbiers and H. T. C. Stoof, Phys. Rev. A **54**, 5055 (1996).

[23] T. Bergeman, Phys. Rev. A **55**, 3658 (1997).

[24] D. A. W. Hutchinson, E. Zaremba, and A. Griffin, Phys. Rev. Lett. **78**, 1842 (1997).

[25] S. Giorgino, L. P. Pitaevskii, and S. Stringari, Phys. Rev. A **54**, R4633 (1996).

[26] M. Houbiers, H. T. C. Stoof, and E. A. Cornell, Phys. Rev. A **56**, 2041 (1997).

[27] This was first pointed out to us by A. J. Leggett.

[28] Ph. Nozières and D. Pines, *The Theory of Quantum Liquids, Volume II: Superfluid Bose Liquids* (Addison-Wesley, New York, 1990).

[29] S. Stringari, Phys. Rev. Lett. **77**, 2360 (1996).

[30] E. Zaremba, A. Griffin, and T. Nikuni (unpublished).

[31] D. S. Jin, J. R. Ensher, M. R. Matthews, C. E. Wieman, and E. A. Cornell, Phys. Rev. Lett. **77**, 420 (1996).

[32] M.-O. Mewes, M. R. Andrews, N. J. van Druten, D. M. Kurn, D. S. Durfee, C. G. Townsend, and W. Ketterle, Phys. Rev. Lett. **77**, 988 (1996).

[33] Yu. Kagan, B. V. Svistunov, and G. V. Shylapnikov, Zh. Éksp. Teor. Fiz. **93**, 552 (1987) [Sov. Phys. JETP **66**, 314 (1987)].

[34] H. T. C. Stoof, A. M. L. Janssen, J. M. V. A. Koelman, and B. J. Verhaar, Phys. Rev. A **39**, 3157 (1989).

[35] E. A. Burt, R. W. Ghrist, C. J. Myatt, M. J. Holland, E. A. Cornell, and C. E. Wieman, Phys. Rev. Lett. **79**, 337 (1997).

[36] W. Ketterle and H.-J. Miesner (unpublished).

[37] M.-O. Mewes, M. R. Andrews, N. J. van Druten, D. M. Kurn, D. S. Durfee, and W. Ketterle, Phys. Rev. Lett. **77**, 416 (1996).

[38] J. R. Ensher, D. S. Jin, M. R. Matthews, C. E. Wieman, and E. A. Cornell, Phys. Rev. Lett. **77**, 4984 (1996).